

- forestier qui la relie au Parc National d'Andringitra: L'herpetofauna. *Rech. Dev. Série Sci. Biol.* **15**, 81–97 (1999).
24. Raselimanana, A. P., Rakotomalala, D. & Rakotondraparany, F. Inventaire biologique de la forêt littorale de Tampolo (Fenoarivo Atsinanana). Les reptiles et amphibiens: Diversité et conservations. *Rech. Dev. Série Sci. Biol.* **14**, 183–195 (1998).
25. Raxworthy, C. J., Forstner, M. R. J. & Nussbaum, R. A. Chameleon radiation by oceanic dispersal. *Nature* **415**, 784–787 (2002).
26. ESRI. *ArcAtlas* (Environmental Systems Research Institute, Redlands, California, 1997).
27. New, M., Hulme, M. & Jones, P. A. 1961–1990 *Mean Monthly Climatology of Global Land Areas* (Climatic Research Unit, University of East Anglia, Norwich, 1997).
28. Peterson, A. T. & Cohoon, K. C. Sensitivity of distributional prediction algorithms to geographic data completeness. *Ecol. Mod.* **117**, 159–164 (1999).
29. Anderson, R. P., Lew, D. & Peterson, A. T. Evaluating predictive models of species' distributions: Criteria for selecting optimal models. *Ecol. Mod.* **162**, 211–232 (2003).
30. Anderson, R. P., Laverde, M. & Peterson, A. T. Geographical distributions of spiny pocket mice in South America: Insights from predictive models. *Global Ecol. Biogeogr.* **11**, 131–141 (2002).

Acknowledgements We thank the Malagasy authorities and the University of Antananarivo Department of Animal Biology for their assistance. Fieldwork (C.J.R. and R.A.N.) was supported by Conservation International, Earthwatch, the National Geographic Society, the US National Science Foundation and the World Wide Fund for Nature. This work was supported by NASA and the Center for Biodiversity and Conservation at the American Museum of Natural History.

Competing interests statement The authors declare they have no competing financial interests.

Correspondence and requests for materials should be addressed to C.J.R. (rax@amnh.org).

Presynaptic induction of heterosynaptic associative plasticity in the mammalian brain

Yann Humeau¹, Hamdy Shaban¹, Stephanie Bissière¹ & Andreas Lüthi^{1,2}

¹Friedrich Miescher Institute, Maulbeerstrasse 66, CH-4058 Basel, Switzerland

²Department of Pharmacology/Neurobiology, Biozentrum, University of Basel, Klingelbergstrasse 70, CH-4056 Basel, Switzerland

The induction of associative synaptic plasticity in the mammalian central nervous system classically depends on coincident presynaptic and postsynaptic activity^{1,2}. According to this principle, associative homosynaptic long-term potentiation (LTP) of excitatory synaptic transmission can be induced only if synaptic release occurs during postsynaptic depolarization^{1,2}. In contrast, heterosynaptic plasticity in mammals is considered to rely on activity-independent, non-associative processes^{3–8}. Here we describe a novel mechanism underlying the induction of associative LTP in the lateral amygdala (LA). Simultaneous activation of converging cortical and thalamic afferents specifically induced associative, N-methyl-D-aspartate (NMDA)-receptor-dependent LTP at cortical, but not at thalamic, inputs. Surprisingly, the induction of associative LTP at cortical inputs was completely independent of postsynaptic activity, including depolarization, postsynaptic NMDA receptor activation or an increase in postsynaptic Ca²⁺ concentration, and did not require network activity. LTP expression was mediated by a persistent increase in the presynaptic probability of release at cortical afferents. Our study shows the presynaptic induction and expression of heterosynaptic and associative synaptic plasticity on simultaneous activity of converging afferents. Our data indicate that input specificity of associative LTP can be determined exclusively by presynaptic properties.

Bipolar stimulating electrodes were placed on afferent fibres from the internal capsule (containing thalamic afferents)^{9–11} or from the external capsule (containing cortical afferents)¹² in coronal slices prepared from 3–4-week-old male C57BL/6J mice (Fig. 1a). Whole-cell current-clamp recordings were obtained from projection

neurons in the dorsolateral portion of the LA (Fig. 1a). Low-frequency baseline stimulation in the presence of the GABA_A (γ-aminobutyric acid) receptor antagonist picrotoxin (100 μM) elicited monosynaptic excitatory postsynaptic potentials (EPSPs) of similar amplitudes and slopes at both afferent inputs (thalamic, 5.6 ± 0.4 mV, 1.07 ± 0.11 mV ms⁻¹; cortical, 5.7 ± 0.4 mV, 1.04 ± 0.11 mV ms⁻¹; n = 13). To mimic the physiological activity of converging thalamic and cortical afferents during fear conditioning^{13,14}, both afferents were stimulated simultaneously for 1.5 s at an average frequency of 30 Hz using two different stimulation protocols containing Poisson-distributed stimuli ('Poisson-train'; Fig. 1b; see Methods). Simultaneous Poisson-train stimulation resulted in the induction of LTP at cortical (151 ± 10% of baseline, n = 13, P < 0.01), but not at thalamic, afferent synapses (98 ± 5%, n = 13, P > 0.05; Fig. 1c). Inverting the two stimulation patterns to assess stimulation protocol-specific effects did not affect the input-specific induction of LTP at cortical input synapses (cortical, 152 ± 16% of baseline, n = 6, P < 0.05; thalamic, 106 ± 12%, n = 6, P > 0.05). The induction of LTP was associative, in that stimulation of both the thalamic and cortical afferents was required. Stimulation of either pathway on its own did not induce LTP at cortical afferents (cortical, 106 ± 15% of baseline, n = 6, P > 0.05; thalamic, 101 ± 8%, n = 5, P > 0.05; Fig. 1d), or at thalamic afferents (cortical, 100 ± 8% of baseline, n = 7, P > 0.05; thalamic, 105 ± 16%, n = 5, P > 0.05; see Supplementary Information), indicating that the stimulation protocols applied were below threshold for the induction of homosynaptic^{10–12} and heterosynaptic LTP at cortical afferents.

Associative LTP in the hippocampus² and the amygdala^{11,12} depends largely on the activation of NMDA receptors and an increase in the postsynaptic Ca²⁺ concentration. Accordingly, heterosynaptic, associative LTP (LTP_{HA}) at cortical afferents could not be induced in the presence of the competitive NMDA receptor antagonist 3-(±)-2-carboxypiperazin-4-yl-propyl-1-phosphonic acid (CPP) at 20 μM (control, 151 ± 10% of baseline, n = 13; CPP, 88 ± 8% of baseline, n = 9, P > 0.05; Fig. 2a). To assess whether NMDA receptor activation in conjunction with Poisson-train stimulation of cortical afferents was sufficient for the induction of LTP_{HA}, we applied NMDA locally in the vicinity of the projection neuron from which we were recording by using a pressure application system. Whereas puff-application of NMDA in the absence of cortical afferent activity did not result in the induction of LTP_{HA} (98 ± 4% of baseline, n = 5, P > 0.05; Fig. 2b), combining the application of NMDA with Poisson-train stimulation of cortical afferents resulted in a potentiation of cortical afferent synapses (157 ± 12% of baseline, n = 4, P < 0.05; Fig. 2b). In contrast, pairing NMDA application with Poisson-train stimulation of thalamic afferents did not induce LTP at thalamic afferents (99 ± 10% of baseline, n = 3, P > 0.05; Fig. 2b).

To determine whether an increase in postsynaptic Ca²⁺ concentration was required for LTP_{HA} induction we dialysed the postsynaptic neuron with the Ca²⁺ chelator BAPTA (10–50 mM). Surprisingly, postsynaptic dialysis with BAPTA did not prevent the induction of LTP_{HA} (152 ± 17% of baseline, n = 14, P < 0.05; Fig. 2c). Given that activation of NMDA receptors is required for the induction of LTP_{HA}, this finding suggests that they are not located on the postsynaptic neuron or, alternatively, that they can signal in a Ca²⁺-independent way. To test these possibilities we dialysed the postsynaptic cell with the NMDA receptor open-channel blocker MK-801, and stimulated cortical and thalamic afferents while holding the postsynaptic cell at +30 mV (ref. 15). This procedure completely blocked postsynaptic NMDA receptors (Fig. 2d). However, even the complete blockade of postsynaptic NMDA receptors did not interfere with the induction of LTP_{HA} (134 ± 9% of baseline, n = 4, P < 0.05; Fig. 2d). To test whether Ca²⁺ signalling was required, we next incubated the slices with BAPTA-acetoxymethyl ester (BAPTA-AM; 50 μM), a membrane-

permeant form of the Ca^{2+} chelator BAPTA. BAPTA-AM completely abolished LTP_{HA} induction ($86 \pm 8\%$ of baseline, $n = 7$, $P > 0.05$; Fig. 2e). In conclusion, the induction of LTP_{HA} was independent of postsynaptic activity including depolarization, postsynaptic NMDA receptor activation and increase in intracellular Ca^{2+} concentration, but still required NMDA receptor activation and Ca^{2+} signalling.

We considered the possibility that LTP_{HA} induction might represent a network phenomenon involving NMDA receptors located on other neurons within the LA. We therefore sought to decrease network excitability strongly in the LA, a brain structure that is tightly controlled by GABA-mediated inhibition^{16,17}, by application of the GABA_A receptor agonist muscimol (5 μM) during LTP induction. Indeed, heterosynaptic forms of plasticity mediated by network activity have been shown to be strongly reduced by activation of GABA_A receptors^{5,18}. Muscimol clamped the membrane potential at or near the chloride equilibrium potential (Fig. 3a), thereby preventing action potential initiation in all neurons expressing GABA_A receptors, including projection neurons and local inhibitory interneurons^{19–21}. However, LTP_{HA} induction was not affected by the presence of muscimol ($146 \pm 14\%$ of baseline, $n = 6$, $P < 0.05$; Fig. 3b), but we could not exclude the possibility that some unknown factor released by neurons not expressing GABA_A receptors would be required for the induction of LTP_{HA} . To investigate this further, we strongly suppressed network activity by application of the AMPA (α -amino-3-hydroxy-5-methyl-4-isoxazole propionic acid) receptor antagonist NBQX (2,3-dihydroxy-6-nitro-7-sulphamoyl-benzo(f)quinoxaline; 20 μM). However, even when AMPA-receptor-mediated synaptic transmission was completely blocked, LTP_{HA} could still be induced as monitored by NMDA-receptor-mediated excitatory postsynaptic currents (EPSCs) recorded at +30 mV ($122 \pm 8\%$ of baseline, $n = 7$, $P < 0.05$; Fig. 3c). Thus, most parsimoniously, our

data are consistent with the possibility that glutamate released by thalamic afferents might directly activate NMDA receptors located on presynaptic terminals of cortical afferents, a hypothesis supported by electron-microscopic studies indicating the presence of the NMDA receptor subunit NR1 on presynaptic terminals in the LA^{22–24}.

If activation of NMDA receptors on presynaptic terminals of cortical afferents underlies the induction of LTP_{HA} , this raises the question why Poisson-train stimulation of cortical afferents alone does not induce LTP. One possible explanation is that glutamate released at cortical afferents would be rapidly cleared by glutamate uptake. Indeed, we found that a single Poisson-train stimulation of cortical afferents was able to induce LTP in the presence of a low concentration of the glutamate uptake blocker TBOA (*D,L-threo*- β -benzyloxyaspartate; 20 μM ; $133 \pm 9\%$ of baseline, $n = 5$, $P < 0.05$; Fig. 3d). To assess whether the facilitation of LTP induction at cortical afferents in the presence of TBOA was due to the activation of presynaptic NMDA receptors by increased ambient glutamate levels, we checked whether TBOA affected the presynaptic properties of cortical afferents (see below) or spontaneous excitatory network activity. However, TBOA did not significantly affect paired-pulse facilitation (PPF) at cortical afferents (control, 1.35 ± 0.15 ; TBOA, 1.44 ± 0.22 ; $n = 3$, $P > 0.05$) or the frequency of spontaneous EPSPs (control, 3.0 ± 0.7 Hz; TBOA, 3.2 ± 1.1 Hz; $n = 5$, $P > 0.05$).

Given the induction mechanism of LTP_{HA} , we reasoned that thalamic afferent stimulation should affect presynaptic function of cortical afferents in an NMDA-receptor-dependent manner. We therefore compared PPF²⁵ in response to double stimulation of cortical afferents (inter-stimulus interval 50 ms) before and after tetanic stimulation (45 stimuli at 30 Hz) of thalamic afferents. Tetanic stimulation of thalamic afferents resulted in a transient decrease in PPF at cortical afferents ($82 \pm 6\%$ of baseline, $n = 7$,

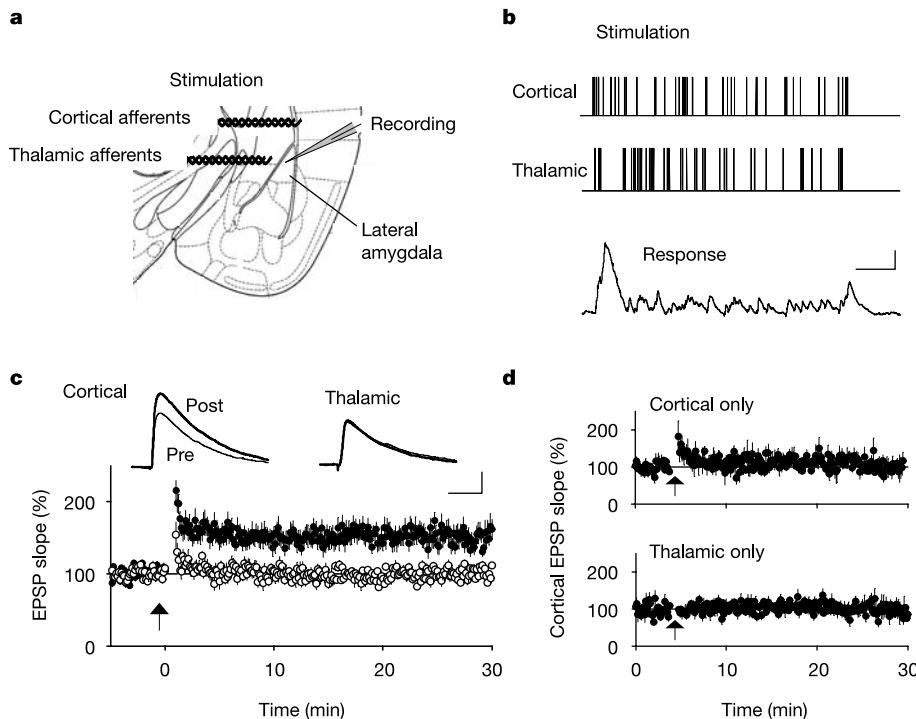


Figure 1 Induction of LTP_{HA} at cortical, but not at thalamic, afferent synapses by simultaneous Poisson-train stimulation of thalamic and cortical afferents. **a**, Placement of stimulating and recording electrodes. **b**, Poisson-train stimulation used for LTP induction. Each train consisted of 45 stimuli at an average frequency of 30 Hz. The trace shows a typical postsynaptic response. Scale bars, 10 mV and 250 ms. **c**, Time course of synaptic

changes after simultaneous Poisson-train stimulation (arrow) of cortical (filled circles) and thalamic (open circles) afferents. Scale bars, 2 mV and 50 ms. **d**, Time course of synaptic changes occurring at cortical afferent synapses upon Poisson-train stimulation (arrow) of either cortical or thalamic afferents alone.

$P < 0.05$; Fig. 4a–c). In contrast, tetanic stimulation of cortical afferents did not affect PPF at thalamic afferents ($104 \pm 4\%$ of baseline, $n = 5$, $P > 0.05$; Fig. 4c). Furthermore, the decrease in cortical PPF after thalamic afferent stimulation was completely

abolished by the NMDA receptor antagonist CPP ($20 \mu\text{M}$; $107 \pm 5\%$ of baseline, $n = 6$, $P > 0.05$; Fig. 4a, c). These results indicate that repeated stimulation of thalamic afferents transiently increases the probability of release (P_r) at cortical afferents in an

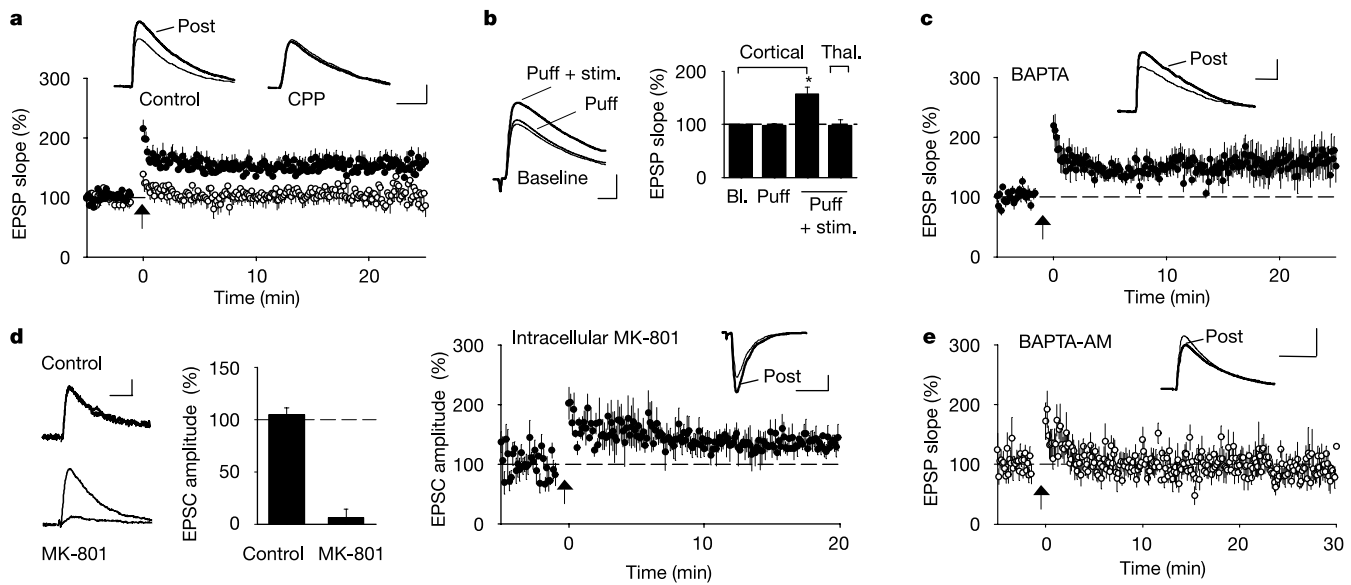


Figure 2 Induction of LTP_{HA} does not depend on postsynaptic activity, but is dependent on NMDA receptor activation and Ca^{2+} . **a**, Induction of LTP_{HA} is blocked in NMDA receptor antagonist CPP (control, same data as in Fig. 1c). Filled circles, control; open circles, CPP. Scale bars, 2 mV and 50 ms. **b**, Left, averaged EPSPs from 2 min of baseline, after pressure application of NMDA (Puff), and 25 min after pairing of NMDA application with cortical afferent stimulation (Puff + stim.). Scale bars, 2 mV and 25 ms. Right, changes in EPSP slope induced by pressure application of NMDA alone, and in conjunction with Poisson-train stimulation of cortical or thalamic afferents. **c**, Induction of LTP_{HA} is

independent of increase in postsynaptic Ca^{2+} . Scale bars, 2 mV and 50 ms. **d**, Left, intracellular dialysis with MK-801 blocks NMDA-receptor-mediated EPSCs recorded at +30 mV in the presence of NBQX. Traces show averaged NMDA EPSCs for the first and last five stimulations. Scale bars, 20 pA and 100 ms. Middle, MK-801-induced blockade of NMDA-receptor-mediated EPSCs at cortical and thalamic afferents (pooled data). Right, LTP_{HA} is not affected by blockade of postsynaptic NMDA receptors. Scale bars, 50 pA and 20 ms. **e**, Induction of LTP_{HA} is blocked in the presence of BAPTA-AM. Scale bars, 2 mV and 50 ms.

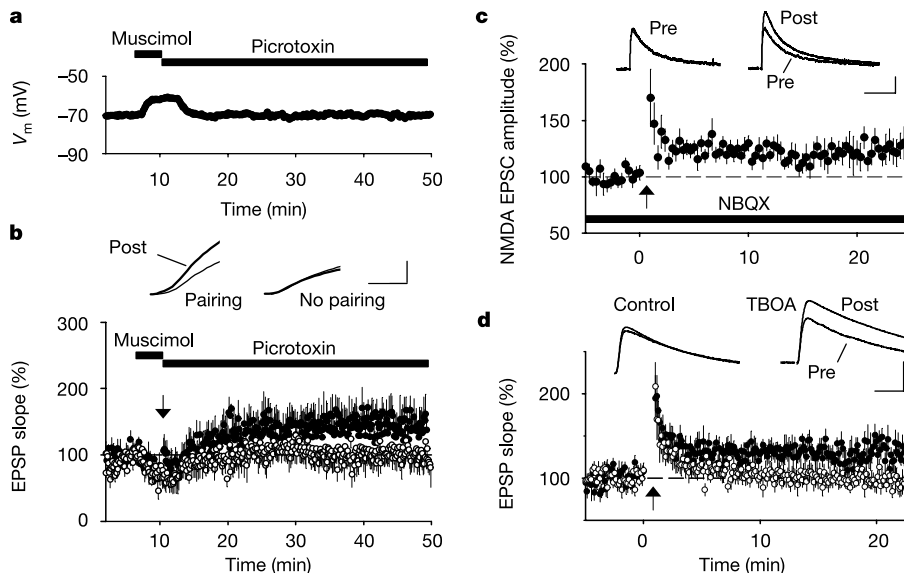


Figure 3 Network activity is not required for the induction of LTP_{HA} . **a**, Average time course of the membrane potential (V_m) during muscimol application. **b**, Induction of LTP_{HA} in the presence of muscimol. Time course of cortical EPSP slope after Poisson-train stimulation and in the absence of Poisson-train stimulation. Picrotoxin was used to terminate shunting induced by tonic GABA_A receptor activation. Filled circles, pairing;

open circles, no pairing. Scale bars, 1.3 mV and 2 ms. **c**, Induction of LTP_{HA} in the presence of NBQX. The plot shows a time course of NMDA-receptor-mediated EPSCs at cortical afferents recorded at +30 mV. Scale bars, 20 pA and 100 ms. **d**, Induction of homosynaptic LTP at cortical afferents in the presence of the glutamate uptake blocker TBOA. Open circles, control; filled circles, TBOA. Scale bars, 3 mV and 25 ms.

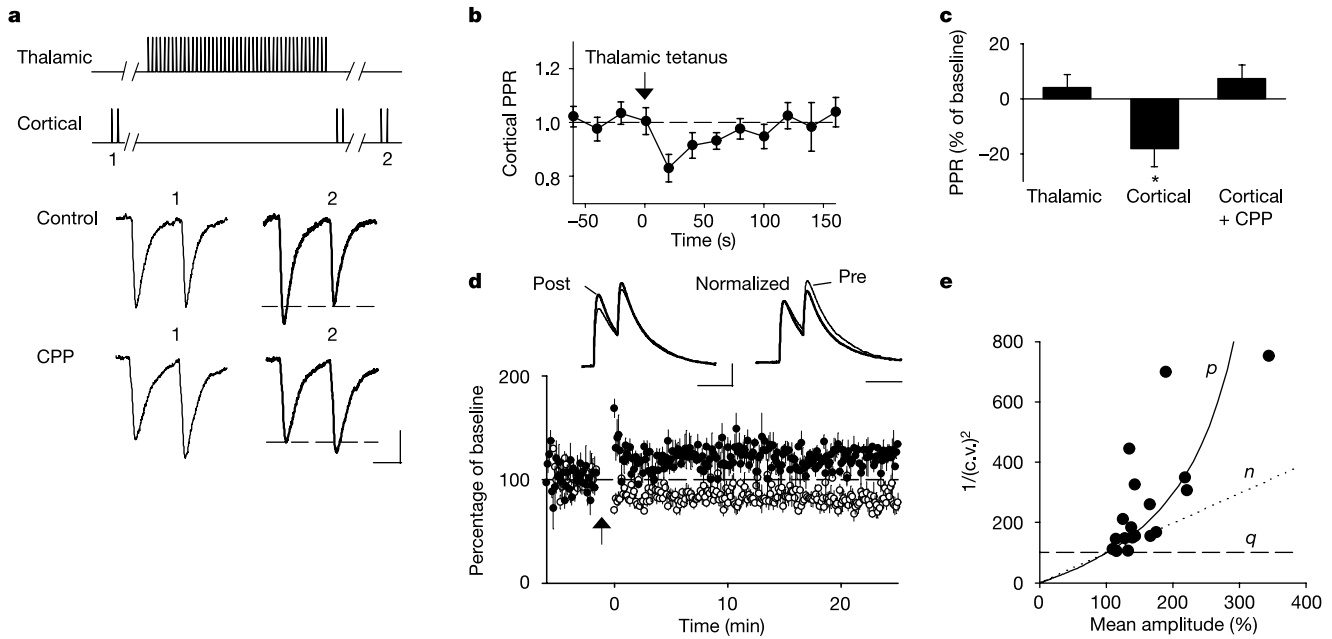


Figure 4 Heterosynaptic, NMDA-receptor-dependent increase of release probability at cortical afferents after stimulation of thalamic afferents. **a**, Top, stimulation protocols. Bottom, EPSCs recorded in response to paired-pulse stimulation (50-ms inter-stimulus interval) of cortical afferents before (point 1) and 10 s after (point 2) tetanic stimulation of thalamic afferents in control conditions or in the presence of CPP. Dashed lines represent the initial amplitude (point 1) of the first response before thalamic stimulation. Scale bars,

40 pA and 20 ms. **b**, Average time course of PPF changes at cortical afferent synapses after tetanic stimulation of thalamic afferents. **c**, PPF changes at thalamic and at cortical afferents after tetanic stimulation of the other input. **d**, Average time course of cortical EPSP slope (filled circles) and PPF (open circles) after induction of LTP_{HA}. Scale bars, 2.5 mV and 75 ms. **e**, Variance analysis of EPSP amplitude fluctuations illustrating that LTP_{HA} expression fits best with an increase in the probability of release (*p*).

NMDA-receptor-dependent manner and that the expression of LTP_{HA} might involve a more persistent increase in P_r at cortical synapses. Indeed, LTP_{HA} was associated with a persistent decrease in PPF ($81 \pm 5\%$ of baseline, $n = 6$, $P < 0.05$; Fig. 4d). Moreover, if LTP_{HA} expression were mediated by an increase in P_r , we reasoned that it should be occluded at high initial P_r . Therefore, we increased P_r by increasing the extracellular Ca^{2+} concentration from 2 to 8 mM. This induced an increase in EPSP amplitude to $175 \pm 19\%$ ($n = 8$, $P < 0.05$) and occluded the further induction of LTP_{HA} after adjusting EPSP amplitude to control values ($111 \pm 11\%$ of baseline, $n = 5$, $P > 0.05$). Finally, using analysis of fluctuations of the postsynaptic response amplitude, we determined the quantal parameters modified upon induction of LTP_{HA} (refs 26, 27). The plot of $1/(c.v.)^2$ (where c.v. is the coefficient of variation) against mean response amplitude shows that LTP_{HA} induction fits best with an increase in P_r (Fig. 4e). Finally, because $1/(c.v.)^2$ is independent of the quantal amplitude (*q*), we directly assessed possible changes in *q* by monitoring the amplitude of asynchronously released quanta in the presence of Sr^{2+} under control conditions and after the induction of LTP_{HA}. The amplitude of stimulation-induced miniature EPSCs at cortical afferents was not significantly affected by the induction of LTP_{HA} (control, -6.7 ± 0.2 pA; LTP, -7.4 ± 1.1 pA; $n = 4$, $P > 0.05$). Because homosynaptic LTP at cortical afferent synapses has previously been shown to be mediated by a presynaptic increase in P_r (refs 12, 26), our results indicate that heterosynaptic LTP_{HA} could share the same expression mechanism. Indeed, we found that the prior induction of homosynaptic LTP by pairing afferent stimulation at 2 Hz with postsynaptic depolarization^{12,26} occluded the subsequent induction of LTP_{HA} using Poisson-train stimulation (see Supplementary Information). However, in contrast to the induction of homosynaptic LTP, which depends on postsynaptic NMDA receptor activation and can be blocked by postsynaptic BAPTA (30 mM; $103 \pm 10\%$ of baseline, $n = 5$)^{12,26},

LTP_{HA} is induced and expressed presynaptically.

The physiological relevance of LTP_{HA} for fear learning is supported by two observations. First, thalamic and cortical afferents to the lateral amygdala are simultaneously active during fear conditioning and can interact^{9,28}. Second, electrophysiological experiments *in vivo* show that postsynaptic hyperpolarization does not completely abolish LTP induced by pairing of sensory stimulation with foot-shocks¹⁴, suggesting that LTP induction independent of postsynaptic activity does occur *in vivo*. The physiological stimulation patterns used in this study suggest that LTP_{HA} might be induced on subthreshold activity elicited by simultaneous sensory input by means of thalamic and cortical afferents. LTP_{HA} might therefore serve as a priming mechanism to increase the impact of selective cortical afferents on the subsequent induction of homosynaptic hebbian plasticity at neighbouring synapses, which requires stronger afferent activity and/or the induction of postsynaptic action potentials^{10–12,20,29,30}.

Our study indicates that the input specificity of associative LTP can be entirely determined by presynaptic properties. Heterosynaptic associative modifications of synaptic efficacy add a level of complexity to the classical hebbian forms of synaptic plasticity, and open a new perspective for understanding integrative processes between converging afferent pathways in the mammalian central nervous system. □

Methods

Coronal slices from 3–4-week-old male C57BL/6J mice were prepared as described²⁰. Slices were maintained for 45 min at 35 °C in an interface chamber containing artificial cerebrospinal fluid equilibrated with 95% O₂/5% CO₂ and containing (in mM): 124 NaCl, 2.7 KCl, 2 CaCl₂, 1.3 MgCl₂, 26 NaHCO₃, 0.4 NaH₂PO₄, 10 glucose, 4 ascorbate; and then kept for at least 45 min at 21–25 °C before being transferred to a superfusing recording chamber. Whole-cell recordings were performed at 30–32 °C. Neurons were identified visually with infrared videomicroscopy. Patch electrodes (3–5 MΩ) were normally filled with a solution containing (in mM): 120 potassium gluconate, 20 KCl, 10 HEPES, 10 phosphocreatine, 4 Mg-ATP, 0.3 Na-GTP, pH 7.25, 295 mOsm. All experiments were

performed in the presence of picrotoxin (100 μ M) unless indicated otherwise. Monosynaptic EPSPs exhibiting constant 10–90% rise times and latencies were elicited by stimulation of afferent fibres with a bipolar twisted platinum/10% iridium wire (25 μ m diameter). LTP was quantified for statistical comparisons by normalizing and averaging EPSP slopes during the last 10 min of experiments relative to 5–10 min of baseline. Depicted traces show averaged EPSPs or EPSCs for 2 min of baseline and 2 min of LTP (20–25 min after pairing). All values are expressed as means \pm s.e.m. Statistical comparisons were done with paired or unpaired Student's *t*-test as appropriate (two-tailed *P* < 0.05 was considered significant). For details on experimental conditions and analysis see Supplementary Information.

Received 18 August; accepted 24 October 2003; doi:10.1038/nature02194.

1. Gustafsson, B. & Wigström, H. Basic features of long-term potentiation in the hippocampus. *Semin. Neurosci.* **2**, 321–333 (1990).
2. Bliss, T. V. P. & Collingridge, G. L. A synaptic model of memory: long-term potentiation in the hippocampus. *Nature* **361**, 31–39 (1993).
3. Bailey, C. H., Giustetto, M., Huang, Y. Y., Hawkins, R. D. & Kandel, E. R. Is heterosynaptic modulation essential for stabilizing Hebbian plasticity and memory? *Nature Rev. Neurosci.* **1**, 11–20 (2000).
4. Artola, A. & Singer, W. Long-term depression of excitatory synaptic transmission and its relationship to long-term potentiation. *Trends Neurosci.* **16**, 480–487 (1993).
5. Scanziani, M., Malenka, R. C. & Nicoll, R. A. Role of intercellular interactions in heterosynaptic long-term depression. *Nature* **380**, 446–450 (1996).
6. Tsukamoto, M. *et al.* Mossy fibre synaptic NMDA receptors trigger non-Hebbian long-term potentiation at entorhino-CA3 synapses in the rat. *J. Physiol. (Lond.)* **546**, 665–675 (2003).
7. Royer, S. & Paré, D. Conservation of total synaptic weight through balanced synaptic depression and potentiation. *Nature* **422**, 518–522 (2003).
8. Nishiyama, M., Hong, K., Mikoshiba, K., Poo, M. M. & Kato, K. Calcium stores regulate the polarity and input-specificity of synaptic modification. *Nature* **408**, 584–588 (2000).
9. LeDoux, J. E. Emotion circuits in the brain. *Annu. Rev. Neurosci.* **23**, 155–184 (2000).
10. Weisskopf, M. G., Bauer, E. P. & LeDoux, J. E. L-type voltage gated calcium channels mediate NMDA-independent associative long-term potentiation at thalamic input synapses to the amygdala. *J. Neurosci.* **19**, 10512–10519 (1999).
11. Bauer, E. P., Schafe, G. E. & LeDoux, J. E. NMDA receptors and L-type voltage gated calcium channels contribute to long-term potentiation and different components of fear memory formation in the lateral amygdala. *J. Neurosci.* **22**, 5239–5249 (2002).
12. Huang, Y. Y. & Kandel, E. R. Postsynaptic induction and PKA-dependent expression of LTP in the lateral amygdala. *Neuron* **21**, 169–178 (1998).
13. Quirk, G. J., Armony, J. L. & LeDoux, J. E. Fear conditioning enhances different temporal components of tone-evoked spike trains in auditory cortex and lateral amygdala. *Neuron* **19**, 613–624 (1997).
14. Rosenkranz, J. A. & Grace, A. A. Dopamine-mediated modulation of odour-evoked amygdala potentials during pavlovian conditioning. *Nature* **417**, 282–287 (2002).
15. Berretta, N. & Jones, R. S. Tonic facilitation of glutamate release by presynaptic N-methyl-D-aspartate autoreceptors in the entorhinal cortex. *Neuroscience* **75**, 339–344 (1996).
16. Lang, E. J. & Paré, D. Similar inhibitory processes dominate the responses of cat lateral amygdaloid projection neurons to their various afferents. *J. Neurophysiol.* **77**, 341–352 (1997).
17. Szinyei, C., Heinbockel, T., Montagne, J. & Pape, H. C. Putative cortical and thalamic inputs elicit convergent excitation in a population of GABAergic interneurons of the lateral amygdala. *J. Neurosci.* **20**, 8909–8915 (2000).
18. Abraham, W. C. & Wickens, J. R. Heterosynaptic long-term depression is facilitated by blockade of inhibition in area CA1 of the hippocampus. *Brain Res.* **546**, 336–340 (1991).
19. Lang, E. J. & Paré, D. Synaptic responsiveness of interneurons of the cat lateral amygdaloid nucleus. *Neuroscience* **83**, 877–889 (1998).
20. Bissière, S., Humeau, Y. & Lüthi, A. Dopamine gates LTP induction in lateral amygdala by suppressing feedforward inhibition. *Nature Neurosci.* **6**, 587–592 (2003).
21. McDonald, A. J. & Mascagni, F. Immunohistochemical localization of the β 2 and β 3 subunits of the GABA_A receptor in the basolateral amygdala of the rat and monkey. *Neuroscience* **75**, 407–419 (1996).
22. Farb, C. R., Aoki, C. & LeDoux, J. E. Differential localization of NMDA and AMPA receptor subunits in the lateral and basal nuclei of the amygdala: a light and electron microscopic study. *J. Comp. Neurol.* **362**, 86–108 (1995).
23. Gracy, K. N. & Pickel, V. M. Ultrastructural localization of NMDAR1 glutamate receptor immunoreactivity in the extended amygdala. *J. Comp. Neurol.* **362**, 71–85 (1995).
24. Farb, C. R. & LeDoux, J. E. Afferents from the rat temporal cortex synapse on lateral amygdala neurons that express AMPA and NMDA receptors. *Synapse* **33**, 218–229 (1999).
25. Hess, G., Kuhnt, U. & Voronin, L. L. Quantal analysis of paired-pulse facilitation in guinea pig hippocampal slices. *Neurosci. Lett.* **77**, 187–192 (1987).
26. Tsvetkov, E., Carlezon, W. A., Benes, F. M., Kandel, E. R. & Bolshakov, V. Y. Fear conditioning occludes LTP-induced presynaptic enhancement of synaptic transmission in the cortical pathway to the lateral amygdala. *Neuron* **34**, 289–300 (2002).
27. Humeau, Y., Popoff, M. R., Kojima, H., Doussau, F. & Poulain, B. Rac GTPase plays an essential role in exocytosis by controlling the fusion competence of release sites. *J. Neurosci.* **22**, 7968–7981 (2002).
28. Doyère, V., Schafe, G. E., Sigurdsson, T. & LeDoux, J. E. Long-term potentiation in freely moving rats reveals asymmetries in thalamic and cortical inputs to the lateral amygdala. *Eur. J. Neurosci.* **17**, 2703–2715 (2003).
29. Markram, H., Lübke, J., Frotscher, M. & Sakman, B. Regulation of synaptic efficacy by coincidence of postsynaptic APs and EPSPs. *Science* **75**, 213–215 (1997).
30. Blair, H. T., Schafe, G. E., Bauer, E. P., Rodrigues, S. M. & LeDoux, J. E. Synaptic plasticity in the lateral amygdala: a cellular hypothesis of fear conditioning. *Learn. Mem.* **8**, 229–242 (2001).

Supplementary Information accompanies the paper on www.nature.com/nature.

Acknowledgements We thank B. Gähwiler, C. Heuss, A. Matus, B. Poulain and E. Seifritz for discussions and comments on the manuscript. This work was supported by the Borderline Personality Disorder Research Foundation, the Swiss National Science Foundation and the Novartis Research Foundation.

Competing interests statement The authors declare that they have no competing financial interests.

Correspondence and requests for materials should be addressed to A.L. (andreas.luthi@fmi.ch).

.....

A microRNA controlling left/right neuronal asymmetry in *Caenorhabditis elegans*

Robert J. Johnston Jr & Oliver Hobert

Department of Biochemistry and Molecular Biophysics, Center for Neurobiology and Behavior, Columbia University, College of Physicians and Surgeons, 701 W.168th Street, New York, New York 10032, USA

.....

How left/right functional asymmetry is layered on top of an anatomically symmetrical nervous system is poorly understood. In the nematode *Caenorhabditis elegans*, two morphologically bilateral taste receptor neurons, ASE left (ASEL) and ASE right (ASER), display a left/right asymmetrical expression pattern of putative chemoreceptor genes that correlates with a diversification of chemosensory specificities^{1,2}. Here we show that a previously undefined microRNA termed *lisy-6* controls this neuronal left/right asymmetry of chemosensory receptor expression. *lisy-6* mutants that we retrieved from a genetic screen for defects in neuronal left/right asymmetry display a loss of the ASEL-specific chemoreceptor expression profile with a concomitant gain of the ASER-specific profile. A *lisy-6* reporter gene construct is expressed in less than ten neurons including ASEL, but not ASER. *lisy-6* exerts its effects on ASEL through repression of *cog-1*, an Nkx-type homeobox gene, which contains a *lisy-6* complementary site in its 3' untranslated region and that has been shown to control ASE-specific chemoreceptor expression profiles³. *lisy-6* is the first microRNA to our knowledge with a role in neuronal patterning, providing new insights into left/right axis formation.

Bilateral symmetry is a common feature of nervous system anatomy across phylogeny. Morphological symmetry is contrasted by the lateralization of many different nervous system functions, as well as by left/right asymmetrical patterns of gene expression^{4–6}. However, in only a very few cases have these asymmetrical gene expression patterns been specifically correlated with functional lateralization. One such example is provided by a bilaterally symmetrical class of taste receptor neurons, the ASE class^{7,8}, which displays left/right asymmetrical expression patterns of a family of putative chemoreceptors with guanylyl cyclase activity (Fig. 1a). In adult animals, the guanylyl cyclase receptor genes *gcy-6* and *gcy-7* are only expressed in ASEL, whereas *gcy-5* is only expressed in ASER¹. The asymmetry of *gcy* gene expression patterns correlates with a functional asymmetry of the ASEL and ASER neurons exemplified by their sensation of a different spectrum of chemosensory cues². The differential segregation of the chemosensory capacities in the left and right ASE neurons is required for intact behaviour in complex sensory environments. In mutant animals that exhibit a partial lateralization of chemoreceptor expression, chemosensation *per se* is unaffected, yet the ability to discriminate between individual chemosensory inputs is lost^{2,9}.

To elucidate how left/right asymmetrical expression of the *gcy*